J. Fluid Mech. (1995), *vol.* 284, *pp.* 43–62

The bath-plug vortex

By LAWRENCE K. FORBES[1] AND GRAEME C. HOCKING[2]

[1] Department of Mathematics, University of Queensland, St. Lucia, Queensland, 4072, Australia

[2] Department of Mathematics, University of Western Australia, Nedlands, Western Australia, 6009, Australia

(Received 15 February 1994 and in revised form 1 September 1994)

Steady flow with constant circulation into a vertical drain is considered. The precise details of the outflow are simplified by assuming that the drain is equivalent to a distributed volume sink, into which the fluid flows with uniform downward speed. It is shown that a maximum outflow rate exists, corresponding to no fluid circulation and vertical entry into the drain hole. Numerical solutions to the full nonlinear problem are computed, using the method of fundamental solutions. An approximate analysis, based on the use of the shallow-water equations, is presented for flows in which the free surface enters the drain. There is, in addition, a second type of solution, having a stagnation point at the free surface and no fluid circulation. These flows are also computed numerically, and results are presented.

1. Introduction

The phenomenon of fluid swirling as it flows out of a bath, through a drain hole at the bottom, is familiar to everyone, and the question of whether the direction of fluid rotation should be clockwise or anticlockwise remains a topic of lively amateur speculation. This paper is concerned with steady irrotational axisymmetric flow of an ideal fluid into a circular drain hole, under the influence of gravity. Circulation is (generally) present in the flow, and as a consequence, the free surface of the fluid is drawn down into the drain hole, at some radius less than the radius of the drain. The outflow therefore occurs through a horizontal annular region, across which the fluid withdrawal speed is assumed to be uniform.

The assumption of steady flow, to be made in this paper, is clearly only an approximation to the real situation existing in the draining of a finite volume of water, such as occurs in the household bath tub, in which the fluid level drops continuously as the bath empties. The steady hypothesis is nevertheless appropriate over certain time intervals, if sufficient fluid is initially present in the bath. Under these circumstances, the draining flow is 'quasi-steady', in the sense that the total flow is characterized by two different timescales, of greatly differing magnitude. One of these is the time taken for transients to die away, and is assumed to be 'small'. The second time constant is the interval required for the entire bath to drain, and is regarded as 'large'. The steady approximation is therefore appropriate over intermediate time intervals between these two extremes.

For intermediate intervals of time, over which the steady hypothesis is justified, it will be assumed that the sides of the bath have no significant influence over the details of the flow in the vicinity of the plug. In this inner region, it will therefore appear as if the flow has effectively been generated in a bath of infinite lateral extent, and this is the situation modelled in this paper. In addition, the flow geometry is assumed to remain axisymmetric; consequently, withdrawal occurs either through a circular or annular drain region at the bottom of the bath.

In this model problem, it is assumed that the fluid is incompressible, inviscid, and flows irrotationally; this circumvents the considerable difficulties associated with computing viscous free-surface flows, and allows the powerful methods of potential theory to be applied. Nevertheless, it is postulated that a constant circulation is present, and this produces the familiar vortex near the plug. In an actual household bath, there is an initial distribution of vorticity in the fluid, usually caused by the manner in which the bath was filled, and this largely accounts for the rotation that is observed, although some additional vorticity might perhaps be produced through viscous shear with boundaries. It will likewise be assumed in the present model that the circulation was generated at the beginning of the experiment. In this way, the important practical problem of swirling flow into a drain will be modelled by means of irrotational flow of an inviscid fluid.

In reality, the precise details of the flow in the outflow drain are extremely complicated, and an understanding of this behaviour involves the solution of a difficult free-surface problem with an outflow jet at infinite depth. In the present three-dimensional problem, such a computation would be extremely difficult, and in any event is not the main focus of the present work. Therefore, a simplifying assumption is made, in which the drain is modelled as a distributed sink of finite area, into which the fluid flows with constant downward velocity component. In the laboratory, this might be achieved using a grate or mesh built across the top of the plug, as is indeed the case in most household baths.

There is now a considerable literature on withdrawal flows, of which the present problem constitutes one aspect. For two-dimensional flows, where fluid is withdrawn through a line sink, Tuck & Vanden-Broeck (1984) were the first investigators to obtain numerical solutions for the fully nonlinear free-surface shape, in the case when the line sink was immersed in a fluid of infinite depth. They obtained an isolated solution at a unique Froude number (dimensionless outflow rate at the sink), for which the free surface of the fluid was drawn down into a vertical cusp. They also hinted at the presence of another branch of solutions having a stagnation point at the free surface, instead of the cusp, but gave no numerical results. These stagnation-type solutions were later found by Hocking & Forbes (1991) and Forbes & Hocking (1993), whose results suggest that there is a maximum limiting Froude number at which some sort of mathematical singularity enters the solution. The work of Tuck & Vanden-Broeck has been extended to the case of two-dimensional flow in fluid of finite depth by Hocking (1985, 1988), and solutions possessing a free-surface cusp were obtained in these cases.

The study of withdrawal flows in three dimensions is considerably more complicated than for the two-dimensional case, at least because the existence of the extra dimension eliminates the possibility of using the powerful conformal mapping techniques on which the two-dimensional solutions rely. Nevertheless, Forbes & Hocking (1990) have considered axisymmetric withdrawal of fluid into a point sink in a fluid of infinite depth, and used an integral-equation approach to obtain solutions in which a stagnation point is present on the free surface, directly above the sink. This work has been extended to the study of unsteady flows by Miloh & Tyvand (1993), in which a careful comparison is made with experimental observations, and Singler & Geer (1993) consider axisymmetric flow in which a point source is located above a gas–liquid interface. A numerical solution of the full unsteady equations of motion has been undertaken by Zhou & Graebel (1990), and their results show either that the free surface may be drawn rapidly into the sink, or else that a re-entrant jet may be formed in the drain.

In this latter case, it is perhaps possible that the eventual steady-state solution that is attained might in fact involve a free-surface stagnation point, as in the work of Forbes & Hocking (1990).

Ivey & Blake (1985) investigated selective withdrawal from a bounded container, in the case when the fluid is continuously stratified with constant density gradient. A similarity analysis of the Boussinesq equations was compared with laboratory results, for axisymmetric geometry, and the evolution in time of the withdrawal layer was studied, with a view to determining the critical Froude number at which this layer collapses into the sink. Earlier work of Lubin & Springer (1967) considered the simpler problem of withdrawal from a stratified fluid with a density discontinuity, and their experimental results show that there is a type of critical Froude number, at which the interface between the two layers enters the sink. The experiments agreed reasonably well with the predictions of an approximate formula based on a simple analysis of the momentum and mass equations. When the upper layer is absent, as in the present paper, this formula suggests that for axisymmetric flow into a circular orifice, the collapse of the withdrawal layer into the sink is approximately independent of the drain radius, and occurs at an approximate Froude number $F \approx (0.69)^{-5/2} = 2.53$. A similar experimental study of axisymmetric withdrawal is described by Jirka & Katavola (1979), in the case when the interface is of finite thickness.

The other complicating feature of three-dimensional withdrawal flows over two-dimensional ones is that new flow behaviours are possible in three dimensions, for which there is no two-dimensional equivalent. The swirling motion of water as it drains from a bath is an obvious example of this extra complexity.

The present problem is concerned with withdrawal flows in three dimensions, for which circulation of the fluid around the drain hole is possible. It is nevertheless assumed that the free surface of the fluid remains axisymmetric, so that there are close similarities with the work of Forbes & Hocking (1990) and a related problem in groundwater flow studied by Forbes, Watts & Chandler (1993*b*). However, it has been observed by Forbes, Hocking & Chandler (1993*a*) that the integral-equation approach of Forbes & Hocking (1990) cannot be applied to axisymmetric problems when the fluid has finite depth, since the integral equation evidently becomes so ill-conditioned that it is of no practical use. This has been found to be the case in the present problem also.

It is therefore necessary to abandon the use of a boundary-integral technique to solve this problem, so that the remaining options for a numerical solution either involve direct methods (such as finite difference or finite element solutions), or else make use of indirect techniques, such as spectral methods. In this paper, a novel type of spectral method is advanced for the solution of this nonlinear problem, in which the velocity potential is expressed in terms of a distribution of singularities placed outside the fluid region. This approach was used successfully by Forbes *et al.* (1993*a*) to solve a related problem involving axisymmetric flow into a point sink on the bottom of the fluid region, when a stagnation point is present at the free surface. In addition, Chandler & Forbes (1994) have shown the use of this method of fundamental singularities in the solution of unsteady free-boundary problems in groundwater flow, and a list of references to this technique may be obtained from their paper.

2. The free-surface problem

Consider a stagnant fluid of depth H and of infinite lateral extent, with a Cartesian coordinate system arranged so that the x- and y-axes lie along the smooth horizontal

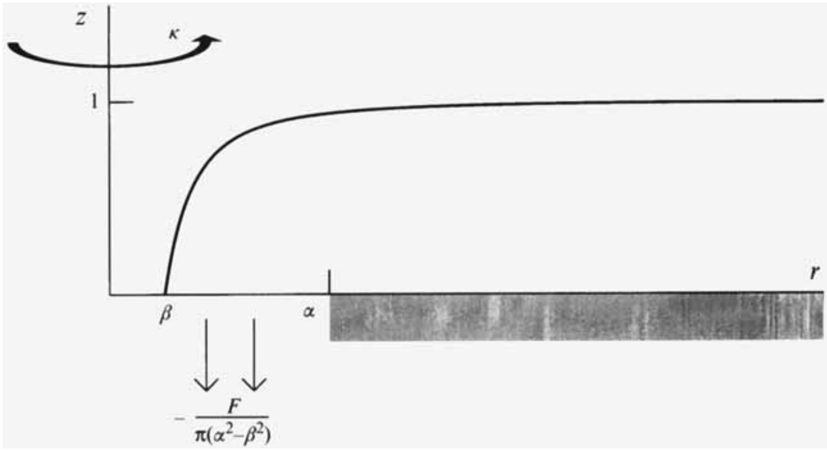

FIGURE 1. A definition sketch of the dimensionless flow. This diagram represents a vertical cross-section through the flow. In view of the axisymmetric geometry, the full situation is obtained by rotation about the z-axis. The bottom of the container is shaded, and the circular drain occupies the region $0 < r < \alpha$. When circulation κ is present about the z-axis, as shown, the free surface enters the drain at radius β. The vertical outflow speed is also indicated.

bottom; the z-axis thus points vertically, as defined by the fact that the acceleration due to gravity, g, acts in the negative z-direction.

Now suppose that a circular drain hole is opened in the bottom, allowing fluid to escape. After transients have died away, a steady flow becomes established, in which a mass flux $\dot{m}$ (mass per unit time) drains from the fluid region. The drain hole is supposed to have radius A, and the free surface of the fluid drops to zero height at some (smaller) inner radius B. The fluid density is ρ, and the swirling motion of the fluid as it leaves through the drain hole is modelled by assuming some constant circulation Γ about the z-axis; in reality, this effect would be the result of an initial distribution of circulation in the fluid. Consequently, the fluid is taken to be incompressible and to flow irrotationally, so that the fluid velocity vector $\boldsymbol{q}$ may be written as the gradient of a velocity potential Φ.

Dimensionless variables are defined, in which all lengths are scaled relative to the depth H of the fluid far from the drain hole, and all velocities are measured against the quantity $(gH)^{1/2}$. A solution to this problem is therefore characterized by the four dimensionless parameters

$$\alpha = \frac{A}{H}, \quad \beta = \frac{B}{H}, \quad F = \frac{\dot{m}}{\rho(gH^5)^{1/2}}, \quad \kappa = \frac{\Gamma}{(gH^3)^{1/2}}.$$

The ratios α and β are respectively the hole radius and the inner radius of the free surface as the fluid leaves the drain. The Froude number F measures the volume flux of fluid down the drain and κ is the dimensionless circulation of the fluid. A sketch of the flow situation in these non-dimensional coordinates is given in figure 1, where the physical significance of the above four parameters is indicated.

Dimensional analysis indicates that the four parameters α, β, F and κ are not independent, but must instead have some functional relationship of the form

$$\mathscr{F}(\alpha, \beta, F, \kappa) = 0.$$

Therefore, it follows that one of these parameters must be determined as part of the solution, and the numerical method of §4 indicates that the circulation κ is most conveniently regarded as the unknown. In a physical experiment, however, it is likely that the circulation κ could be determined in advance, and the inner radius β would be unknown, and so the relationship between β and κ is considered in detail in §7.

In view of the assumed axisymmetry of this problem, it is convenient to introduce cylindrical polar coordinates (r, θ, z) according to the usual definitions $x = r\cos\theta$ and $y = r\sin\theta$. The velocity potential Φ is written in the form

$$\begin{aligned}\Phi &= \frac{\kappa}{2\pi}\arctan\left(\frac{y}{x}\right) + \Phi^R(x,y,z) \\ &= \frac{\kappa\theta}{2\pi} + \Phi^R(r,z),\end{aligned} \tag{2.1}$$

and the incompressibility of the fluid then leads to Laplace's equation

$$\nabla^2\Phi^R = \Phi^R_{rr} + \frac{1}{r}\Phi^R_r + \Phi^R_{zz} = 0, \tag{2.2}$$

for the residual velocity potential Φ^R. The subscripts denote partial derivatives with respect to the indicated variables.

The (axisymmetric) surface of the fluid is represented by the equation $z = \zeta(r)$, and it follows that this function satisfies the constraints

$$\left.\begin{aligned}&\zeta(r) \to 0 \quad \text{as} \quad r \to \beta^+, \\ &\zeta(r) \to 1 \quad \text{as} \quad r \to \infty.\end{aligned}\right\} \tag{2.3}$$

Along this surface, there is a kinematic condition

$$\Phi^R_z = \Phi^R_r \frac{\mathrm{d}\zeta}{\mathrm{d}r} \tag{2.4}$$

which expresses the fact that the fluid may not cross its own bounding surface. In addition, the dynamic requirement that fluid pressure must equal atmospheric pressure on the free surface leads to a Bernoulli equation of the form

$$\frac{1}{2}\left[(\Phi^R_r)^2 + \frac{\kappa^2}{4\pi^2 r^2} + (\Phi^R_z)^2\right] + z = 1 \quad \text{on} \quad z = \zeta(r). \tag{2.5}$$

A detailed description of the flow within the drain is both difficult and unnecessary for the purposes of this paper. Instead, the effect of the outflow pipe is modelled here simply as a region $\beta < r < \alpha$ in which there is uniform outflow speed at the bottom. (This could be achieved approximately in the laboratory by making use of a flow straightening device, such as a grill or a horsehair mat, at the entrance to the drain.) Accordingly, the bottom condition becomes

$$\Phi^R_z = 0 \qquad \text{for} \quad z = 0, \quad r > \alpha, \tag{2.6a}$$

$$\Phi^R_z = -\frac{F}{\pi(\alpha^2 - \beta^2)} \quad \text{for} \quad z = 0, \quad \beta < r < \alpha. \tag{2.6b}$$

It follows from a consideration of the above problem, defined by (2.1)–(2.6), that there must be a limiting Froude number F_L, beyond which solutions of the type sought here are not possible. This result is developed in the theorem which follows.

THEOREM *Solutions to the present problem exist only within the interval of Froude numbers*

$$F \leqslant F_L = \surd 2\pi(\alpha^2 - \beta^2). \tag{2.7}$$

At the limiting Froude number $F = F_L$, the free surface enters the drain vertically, and there is no circulation.

Proof Consider the point $r = \beta$, at which the free surface enters the drain. At that point, the vertical component of fluid velocity is given by the bottom condition (2.6), and is simply $\Phi_z^R = -F/(\pi(\alpha^2-\beta^2))$, as shown in figure 1. By the kinematic condition (2.4) at the free surface, the radial velocity component at the entry point is

$$\Phi_r^R = -\frac{F}{\pi(\alpha^2-\beta^2)(\mathrm{d}\zeta/\mathrm{d}r)} \quad \text{at} \quad r = \beta.$$

Bernoulli's equation (2.5), evaluated at the entry point $r = \beta$, now yields

$$\kappa = 2\pi\beta\left[2-\frac{F^2}{\pi^2(\alpha^2-\beta^2)^2}\left(1+\frac{1}{(\mathrm{d}\zeta/\mathrm{d}r)^2_{r=\beta}}\right)\right]^{1/2}. \tag{2.8}$$

Equation (2.8) shows at once that the circulation κ is bounded, according to the formula

$$\kappa \leqslant \surd 8\pi\beta, \tag{2.9}$$

with the equality sign holding only when no withdrawal through the drain takes place. In addition, it follows from (2.8) that a lower bound exists for the angle of entry of the surface into the drain, since

$$\frac{\mathrm{d}\zeta}{\mathrm{d}r} \geqslant \frac{F}{[2\pi^2(\alpha^2-\beta^2)^2-F^2]^{1/2}} \quad \text{at} \quad r = \beta. \tag{2.10}$$

The restriction (2.7) follows at once from this inequality (2.10), since the argument of the square root must be positive. In addition, if the equality $F = F_L$ holds, then the slope in (2.10) becomes infinite, corresponding to vertical entry, and the circulation κ in (2.8) falls to zero. This completes the proof of the theorem.

Some comments on the physical significance of this theorem are in order. In dimensional variables, the restriction (2.7) becomes

$$\dot{m}/\rho \leqslant (2gH)^{1/2}\pi(A^2-B^2),$$

and this may be understood by a consideration of energy. It follows from the Bernoulli equation (2.5) that the maximum (dimensional) speed at which a fluid particle can enter the drain is $(2gH)^{1/2}$, which is simply equivalent to converting the potential energy of a particle at the free surface, far from the drain, into pure kinetic energy. Furthermore, the circulation must fall to zero if this maximum speed is to be directed vertically downward at the drain. The (dimensional) area of the annular outflow region at the drain is $\pi(A^2-B^2)$, and thus (2.7) is equivalent to a statement that the maximum volume flux out of the drain equals the maximum speed multiplied by the outflow area, as expected. In addition, the maximum can only be achieved with zero circulation.

Similar energy arguments can be used to give the physical meaning of the inequality (2.9), which in dimensional variables, becomes

$$\Gamma/(2\pi B) \leqslant (2gH)^{1/2}.$$

By elementary energy considerations, the maximum possible speed of a fluid particle is $(2gH)^{1/2}$, and inequality (2.9) shows that the speed $\Gamma/(2\pi B)$ induced at radius B by the (dimensional) circulation Γ cannot exceed this upper limit.

At the lower limit $F = 0$, the exact solution to the problem defined by (2.1)–(2.6) is particularly simple to obtain, since this situation corresponds to zero outflow through the drain hole. It is then the case that $\Phi^R = 0$. Bernoulli's equation (2.5) and the formula (2.8) for the circulation then yield the solution

$$\left.\begin{aligned} \zeta(r) &= 1-(\beta/r)^2, \\ \kappa &= \sqrt{8\pi\beta} \quad \text{for} \quad F = 0. \end{aligned}\right\} \tag{2.11}$$

In this case, the free surface intersects the bottom at $r = \beta$ purely as a result of the circulation of the fluid; this effect is familiar to anyone who has spun a shallow dish containing water. Equation (2.11) forms a useful starting solution for the numerical algorithm to be described later.

3. Solution by the method of fundamental singularities

Following Forbes *et al.* (1993*a*), the residual velocity potential Φ^R defined in (2.1) is further split as follows:

$$\Phi^R(r,z) = \Phi^S(r,z) + \chi(r,z). \tag{3.1}$$

In this representation, the function Φ^S is the 'rigid lid' solution, in which the free surface $z = \zeta(r)$ is replaced by the plane $z = 1$, and the term $\chi(r,z)$ provides a local correction near the region of the drain. The advantage of the form (3.1) is that only the function χ is unknown, and it clearly vanishes as $r \to \infty$.

The function Φ^S in (3.1) is computed using the method of images (see, for example, Milne-Thomson 1979). To begin, it is necessary to know the potential $\Phi_0^S(r,z)$ due to a sink that is uniformly distributed over the area between the circles $r = \beta$ and $r = \alpha$ on the plane $z = 0$. The boundary conditions to be satisfied are therefore that $\nabla\Phi_0^S$ should vanish as $z \to \infty$, and that Φ_0^S should satisfy the bottom condition (2.6) exactly. We show in the Appendix that the potential Φ_0^S generates radial and vertical velocity components given by the expressions

$$U_0^S(r,z) = \frac{\partial\Phi_0^S}{\partial r} = \frac{F}{\pi(\alpha^2-\beta^2)}\int_0^\infty [\beta J_1(k\beta) - \alpha J_1(k\alpha)]\, J_1(kr)\, \mathrm{e}^{-k|z|}\, \mathrm{d}k, \tag{3.2a}$$

$$W_0^S(r,z) = \frac{\partial\Phi_0^S}{\partial z} = \frac{F\,\mathrm{sgn}\,(z)}{\pi(\alpha^2-\beta^2)}\int_0^\infty [\beta J_1(k\beta) - \alpha J_1(k\alpha)]\, J_0(kr)\, \mathrm{e}^{-k|z|}\, \mathrm{d}k, \tag{3.2b}$$

in which J_n denotes the Bessel function of the first kind of order n, and $\mathrm{sgn}\,(z)$ is the sign function, which has the values 1 if $z > 0$ and -1 if $z < 0$. From tables of integrals, such as those available in Prudnikov, Brychkov & Marichev (1986), it is possible to evaluate the expressions (3.2) in terms of incomplete elliptic integrals involving rather complicated arguments. As will be seen presently, however, this is of no advantage in the numerical solution, and has not been pursued.

Only the radial and vertical derivatives of the potential function Φ^S in (3.1) are actually required, and these may be obtained from the basic functions (3.2) using the method of images. The solution Φ^S consists of the distributed source on the plane $z = 0$, and an infinite image system on the planes $z = \pm 2m$, $m = 1,2,3,\ldots$, above and below the actual fluid region. Thus the velocity components corresponding to the 'rigid lid' solution Φ^S in (3.1) are

$$U^S(r,z) = \sum_{m=-\infty}^{\infty} U_0^S(r, z-2m), \tag{3.3a}$$

$$W^S(r,z) = \sum_{m=-\infty}^{\infty} W_0^S(r, z-2m). \tag{3.3b}$$

It turns out that the infinite sums in (3.3) may be evaluated in closed form under the integrals that appear in the definitions of the functions U_0^S and W_0^S in (3.2), and the exploitation of this fact confers an enormous advantage in terms of the speed and efficiency of the numerical solution technique. The task reduces to one of summing all positive integral powers of the term $\mu = \exp(-2k)$ for $k > 0$. Since $0 < \mu < 1$, the sums are (uniformly convergent) geometric series, so that the orders of summation and integration may be interchanged. After a little algebra, the 'rigid lid' velocity components in (3.3) may be written

$$U^S(r,z) = \frac{F}{\pi(\alpha^2-\beta^2)}\int_0^\infty e^{-kz}[\beta J_1(k\beta)-\alpha J_1(k\alpha)]\,J_1(kr)\left[\frac{1+e^{-2k(1-z)}}{1-e^{-2k}}\right]dk, \quad (3.4a)$$

$$W^S(r,z) = \frac{F}{\pi(\alpha^2-\beta^2)}\int_0^\infty e^{-kz}[\beta J_1(k\beta)-\alpha J_1(k\alpha)]\,J_0(kr)\left[\frac{1-e^{-2k(1-z)}}{1-e^{-2k}}\right]dk. \quad (3.4b)$$

These expressions are now in a form particularly well suited to numerical evaluation.

It remains to choose an appropriate spectral form for the unknown function $\chi(r,z)$ in the decomposition (3.1). This function is represented in terms of a distribution of ring sinks, placed at points $(\rho, \xi(\rho))$ outside the fluid region, and an image distribution at points $(\rho, -\xi(\rho))$ in order to satisfy the bottom condition $\chi_z(r,0) = 0$ identically. Therefore, it is assumed that

$$\chi(r,z) = \int_0^\infty M(\rho)\int_{-\pi}^{\pi}\{[r^2+\rho^2-2r\rho\cos\theta+(z-\xi)^2]^{-1/2} + [r^2+\rho^2-2r\rho\cos\theta+(z+\xi)^2]^{-1/2}\}\,d\theta\,d\rho, \quad (3.5)$$

and the task is now to determine the source-strength function $M(\rho)$.

It is again the case that only the r- and z-derivatives of the perturbed potential χ in (3.5) are needed in this computation, and for these functions the inner integrals (with respect to θ) can be expressed in terms of complete elliptic integrals. This is of considerable numerical advantage. After very substantial algebra, it may be shown that the radial and vertical derivatives, which give components u and w of a perturbation velocity, can be written in the form

$$u(r,z) = \chi_r = -\int_0^\infty M(\rho)\,[\mathbb{K}(r,\rho,P^{(-)},Q)+\mathbb{K}(r,\rho,P^{(+)},Q)]\,d\rho, \quad (3.6a)$$

$$w(r,z) = \chi_z = -\int_0^\infty M(\rho)\,[(z-\xi)\,\mathbb{L}(P^{(-)},Q)+(z+\xi)\,\mathbb{L}(P^{(+)},Q)]\,d\rho, \quad (3.6b)$$

in which the kernel functions are defined to be

$$\mathbb{K}(r,\rho,P,Q) = \frac{4}{Q(P+Q)^{1/2}}\left[\rho K\left(\frac{2Q}{P+Q}\right)+\frac{rQ-\rho P}{P-Q}E\left(\frac{2Q}{P+Q}\right)\right], \quad (3.7a)$$

$$\mathbb{L}(P,Q) = \frac{4}{(P-Q)(P+Q)^{1/2}}E\left(\frac{2Q}{P+Q}\right). \quad (3.7b)$$

The functions K and E appearing in (3.7a, b) are respectively the complete elliptic integrals of the first and second kinds, as defined by Abramowitz & Stegun (1972, p. 590), and the remaining auxiliary quantities are given by the expressions

$$P^{(\pm)} = r^2+\rho^2+(z\pm\xi)^2, \quad Q = 2r\rho. \quad (3.7c)$$

The derivation of the expressions (3.6) is lengthy, and will not be given here. Details may be found in Forbes *et al.* (1993*a*), and the required transformations are given in the Appendix of the paper by Forbes & Hocking (1990).

4. Numerical methods

The numerical task is to compute approximate values for the free-surface elevation $\zeta(r)$ in (2.3)–(2.5), and for the source-strength function $M(r)$ in the representations (3.6). This is accomplished here using collocation.

The (axisymmetric) free-surface shape is sought at the N numerical mesh points $r_1, r_2, \ldots, r_N$, and the surface elevation and source strength are represented by discrete point values $\zeta_1, \zeta_2, \ldots, \zeta_N$ and $M_1, M_2, \ldots, M_N$ respectively. Here, $r_1 = \beta$ is the point at which the free surface enters the drain, from which it follows that $\zeta_1 = 0$. In addition, we set $M_1 = 0$, and attempt to solve for the $(2N-2)$-vector of unknowns

$$U = [\zeta_2, \ldots, \zeta_N; M_2, \ldots, M_N]^T. \tag{4.1}$$

In this paper, the Froude number F and the drain radius α are given. In addition, it is assumed that the radius β at which the free surface enters the drain is known, so that the circulation κ must be computed as an unknown.

An initial guess is made for the vector U in (4.1); this estimate is updated later using Newton's method. For small Froude numbers F, the zero-outflow solution (2.11) provides a good starting point for the numerical algorithm, and higher Froude numbers can then be explored by boot-strapping from known solutions at smaller Froude numbers. A cubic spline is now fitted through the approximate values of the surface elevation, and differentiated exactly to give the slopes $\zeta'_1, \zeta'_2, \ldots, \zeta'_N$ at all the mesh points. Since a value is now available for the derivative ζ'_1, an estimate for the circulation κ is obtained on the basis of (2.8).

Numerical approximations $U^S_j = U^S(r_j, \zeta_j)$ and $W^S_j = W^S(r_j, \zeta_j)$, $j = 2, 3, \ldots, N$ to the velocity components in (3.4) are next computed. The integrals in these expressions are evaluated to high accuracy, using Gauss–Laguerre quadrature of order 68, with values for the weights and abscissae taken from Stroud & Secrest (1966). In addition, it is necessary to calculate approximate perturbation velocity components $u_j = u(r_j, \zeta_j)$ and $w_j = w(r_j, \zeta_j)$, $j = 2, 3, \ldots, N$ using (3.6). This requires a good choice for the positions $(\rho, \xi(\rho))$ of the source points outside the fluid region. We assume values $\rho_j = r_j$ and $\xi_j = \xi(\rho_j) = \zeta_j + \delta$, $j = 1, 2, \ldots, N$ for an appropriate small positive constant δ. A typical choice for this constant is $\delta = 0.05$. The Bessel functions appearing in (3.4) and the elliptic integrals in (3.7*a*, *b*) are computed to a high order of accuracy by making use of the polynomial approximations given in Abramowitz & Stegun (1972).

The vector (4.1) of unknowns is now updated iteratively, using a damped Newton method. The Bernoulli equation (2.5) and the kinematic surface condition (2.4) are used to construct a residual error vector $E(U)$, also of length $2N-2$, which has components

$$\left.\begin{aligned} E_{j-1} &= 1 - \zeta_j - \frac{1}{2}\left[(U^S_j + u_j)^2 + \frac{\kappa^2}{4\pi^2 r_j^2} + (W^S_j + w_j)^2\right], \qquad &(4.2a)\\ E_{N+j-2} &= (W^S_j + w_j) - (U^S_j + u_j)\,\zeta'_j, &(4.2b) \end{aligned}\right\} \quad j = 2, 3, \ldots, N.$$

A solution for circulating flow into a drain is thus obtained after Newton's method has successfully driven the vector E to within some small pre-determined distance from zero.

5. The predictions of shallow-water theory

For small Froude numbers, it is possible to use the equations of shallow-water theory to give approximate solutions for the free-surface elevation $\zeta(r)$, in the presence of circulation. The resulting expressions have the advantage that they are relatively simple to analyse.

In the shallow-water theory, the vertical component W of velocity is ignored, and the pressure is assumed to behave hydrostatically, according to the formula $p(r,z)=\zeta(r)-z$ in the present non-dimensional variables. The radial velocity component $U(r)$ then becomes approximately independent of depth, and satisfies the (integrated) radial momentum equation

$$\tfrac{1}{2}U^2+\frac{\kappa^2}{8\pi^2r^2}+\zeta=1. \tag{5.1}$$

Conservation of mass is enforced in this theory by integrating the exact continuity equation

$$\frac{\partial(rU)}{\partial r}+\frac{\partial(rW)}{\partial z}=0$$

over depth, between the surfaces $z=0$ and $z=\zeta(r)$. The vertical component W of velocity at the free surface is eliminated using the kinematic condition (2.4), and W on $z=0$ must satisfy the bottom condition (2.6). A further integration of the resulting equation then shows that the mass flux $rU\zeta$ is given by

$$rU\zeta=-\frac{F}{2\pi} \quad \text{for} \quad r>\alpha, \tag{5.2a}$$

$$rU\zeta=-\frac{F(r^2-\beta^2)}{2\pi(\alpha^2-\beta^2)} \quad \text{for} \quad \beta<r<\alpha. \tag{5.2b}$$

Thus the flux is continuous at the rim of the drain hole, $r=\alpha$, and falls to zero at the inner radius $r=\beta$, as expected.

A simple cubic equation for the function $\zeta(r)$ in shallow-water theory can be derived by combining the momentum equation (5.1) and the mass equation (5.2). This gives

$$8\pi^2r^2\zeta^3+(\kappa^2-8\pi^2r^2)\zeta^2+F^2=0 \quad \text{for} \quad r>\alpha, \tag{5.3a}$$

$$8\pi^2r^2\zeta^3+(\kappa^2-8\pi^2r^2)\zeta^2+\frac{(r^2-\beta^2)^2F^2}{(\alpha^2-\beta^2)^2}=0 \quad \text{for} \quad \beta<r<\alpha. \tag{5.3b}$$

The value of the circulation κ in the shallow-water theory can be computed by insisting that the only possible solution to (5.3) at radius $r=\beta$ is $\zeta=0$, as must be the case on physical grounds. Thus it follows that

$$\kappa=\surd 8\pi\beta \tag{5.4}$$

for very shallow flows, exactly as in the case of the zero-withdrawal solution (2.11), (for $F=0$).

The free-surface slope is obtained from (5.3) by differentiation, and becomes

$$\frac{d\zeta}{dr}=\frac{8\pi^2r\zeta^2(1-\zeta)}{\zeta[\kappa^2+4\pi^2r^2(3\zeta-2)]} \quad \text{for} \quad r>\alpha, \tag{5.5a}$$

$$\frac{d\zeta}{dr}=\frac{2r\left[\dfrac{F^2(\beta^2-r^2)}{(\alpha^2-\beta^2)^2}+4\pi^2\zeta^2(1-\zeta)\right]}{\zeta[\kappa^2+4\pi^2r^2(3\zeta-2)]} \quad \text{for} \quad \beta<r<\alpha. \tag{5.5b}$$

It also follows from the differentiated form (5.5) that the circulation κ takes the value (5.4), since the slope $\mathrm{d}\zeta/\mathrm{d}r$ must always be positive for these flows, and this is only possible if

$$\kappa^2+4\pi^2r^2(3\zeta-2) \geqslant 0 \quad \text{for} \quad r \geqslant \beta,$$

with the equality holding at $r=\beta$. In addition, the numerator in (5.5*b*) must be positive for all $r \in (\beta, \alpha)$, since the surface rises monotonically as r increases, and this imposes the constraint

$$F^2 \leqslant \frac{4\pi^2\zeta^2(1-\zeta)(\alpha^2-\beta^2)^2}{(r^2-\beta^2)}.$$

Because the function $\zeta(r)$ satisfies the inequalities $0 \leqslant \zeta \leqslant 1$, it follows that the term $\zeta^2(1-\zeta)$ reaches its maximum value $4/27$ if $\zeta = 2/3$. Allowing $r \rightarrow \alpha$ then yields the result

$$F \leqslant \pi[\tfrac{16}{27}(\alpha^2-\beta^2)]^{1/2}. \tag{5.6}$$

This upper bound (5.6) on the Froude number F is evidently the approximation in shallow-water theory to the exact upper bound F_L given in the condition (2.7).

A Newton method program has been written, to evaluate the surface elevation $\zeta(r)$ as a solution to the cubic equations (5.3).

6. Solutions with a free-surface stagnation point

There is a second branch of possible solutions to this problem, possessing no circulation, and having a stagnation point on the free surface at the centre of the drain $r=0$. Such solutions have been computed by Forbes *et al.* (1993*a*) for the simpler situation in which the drain is replaced by a point sink lying on the bottom $z=0$.

Stagnation-type solutions can be obtained with minor modifications to the numerical methods of §4. Now the free-surface elevation is sought at every numerical mesh point, so that the first point $r_1 = 0$ receives no special treatment. Accordingly, the vector of unknowns (4.1) is replaced with the $2N$-vector

$$U = [\zeta_1, \zeta_2, \ldots, \zeta_N; M_1, M_2, \ldots, M_N]^T. \tag{6.1}$$

The parameter β no longer appears in the formulation of this problem, since it has no meaning for these stagnation solutions.

As in §4, all other quantities at the free surface are now calculated, after some initial guess for the vector U in (6.1) has been made. Of course, no circulation is computed, since (2.8) is not relevant for these flows. The error vector (6.1) is again corrected iteratively, using Newton's method to satisfy the Bernoulli equation (2.5) and the kinematic condition (2.4). The only change this entails is that the residual error vector (4.2) must now be replaced with the $2N$-vector $\boldsymbol{E}(U)$ having components

$$\left.\begin{aligned} E_j &= 1-\zeta_j-\tfrac{1}{2}[(U_j^S+u_j)^2+(W_j^S+w_j)^2], \\ E_{N+j} &= (W_j^S+w_j)-(U_j^S+u_j)\,\zeta_j', \end{aligned}\right\} \quad j=1,2,\ldots,N. \qquad \begin{aligned}(6.2a)\\(6.2b)\end{aligned}$$

Newton's method is used to solve the equation $\boldsymbol{E}(U) = \boldsymbol{0}$.

7. Presentation of results for circulating flow

According to the theorem proved in §2, the branch of solutions of the type in which circulation is present, and the free surface enters the drain, is ultimately limited at a value of Froude number F_L when the circulation falls to zero and the surface becomes

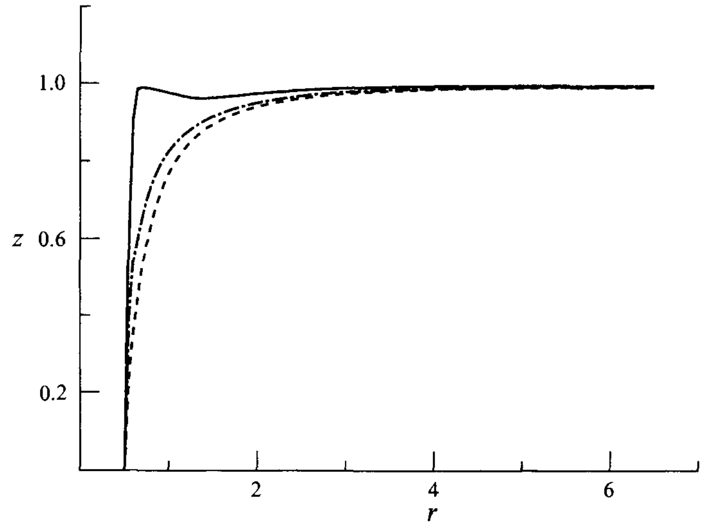

FIGURE 2. Surface profiles for $\alpha = 1$, $\beta = 0.5$, at the three values of Froude number $F = 1$ (dashed line), $F = 2$ (dot-dashed), and $F = 3.3$ (solid line).

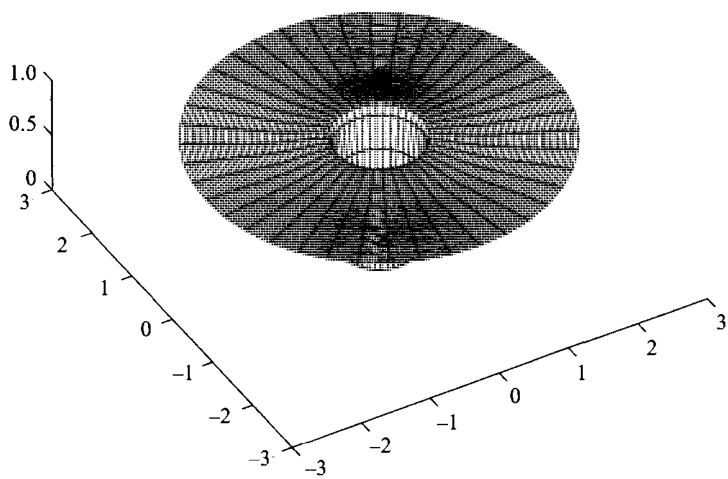

FIGURE 3. A portion of the axisymmetric surface, for $\alpha = 1$, $\beta = 0.5$ and $F = 3.3$.

vertical near the drain. This prediction is now studied using the numerical scheme of §4.

Figure 2 shows surface profiles for three different Froude numbers, all obtained with the same values of the drain radius $\alpha = 1$ and the inner free-surface radius $\beta = 0.5$. The curve sketched with a dashed line corresponds to the surface shape obtained with $F = 1$, and in fact does not differ greatly from the profile given by (2.11) for the case of zero Froude number. The circulation for the solution with $F = 1$ has been determined numerically (from (2.8)) to be $\kappa = 4.231$, and this differs by only about 5% from the value predicted for zero Froude number by (2.11). The solution for $F = 2$, drawn using a dot-dashed line in figure 2, is considerably steeper near the point of entry into the drain, and its circulation has fallen to $\kappa = 3.542$.

The limiting Froude number for this case is obtained from (2.7) and has the value

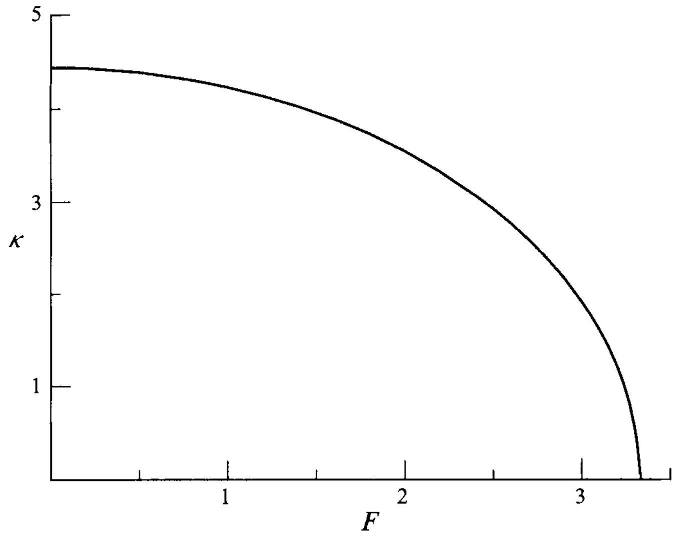

FIGURE 4. The circulation κ as a function of the Froude number F for swirling flow into the drain. Here, $\alpha = 1$ and $\beta = 0.5$.

$F_L = 3.3322$. We have been able to obtain numerical solutions up to about $F = 3.32$, beyond which the Newton method algorithm of §4 breaks down. A surface profile for $F = 3.3$ is also sketched in figure 2 (with a solid line), and the circulation for this solution is found to be $\kappa = 0.5304$. The free-surface slope near the entry point $r = \beta$ has become extremely large, to the extent that a certain granularity, due to the finite mesh of numerical points, may possibly be noticeable in portions of the surface. In addition, a dip has now appeared in the free surface, similar to that observed in the other branch of solutions to this problem, in which a stagnation point is present on the surface; results for this type of solution are discussed in the next section. It is possible that the limiting solution in this case might also form a stagnation point at the surface, near $(r, z) = (\beta, 1)$.

It is of course the case that the solutions shown in figure 2 represent a cross-section of the actual free surface, which is axisymmetric about the z-axis. To emphasize this point, a portion of the solution for $F = 3.3$ sketched in figure 2 is drawn in three-dimensional form in figure 3. The abrupt rise of the free surface near the drain is apparent, as is the small dip that follows it.

In figure 4, the dependence of the circulation κ upon the Froude number F is shown, for the same case as in figure 2, in which the drain radius is $\alpha = 1$ and the radius of the entry point of the surface into the sink is $\beta = 0.5$. The intersection point of the curve shown with the κ-axis (corresponding to $F = 0$) has been computed from (2.11), and the other end of this solution branch, intersecting the F-axis at $F = 3.3322$ (where $\kappa = 0$) is known from (2.7) and the accompanying theorem. These two points are linked by the numerically generated branch of solutions shown in the diagram. For small F there is little change in the value of circulation predicted by the zero Froude number solution (2.11), as observed in figure 2, but as the Froude number is increased to its maximum value F_L given by (2.7), the circulation decreases abruptly.

For small Froude numbers, the free-surface profiles computed numerically are in good agreement with the predictions of the shallow-water theory detailed in §5. As Froude number is increased, shallow-water theory performs less well in comparison

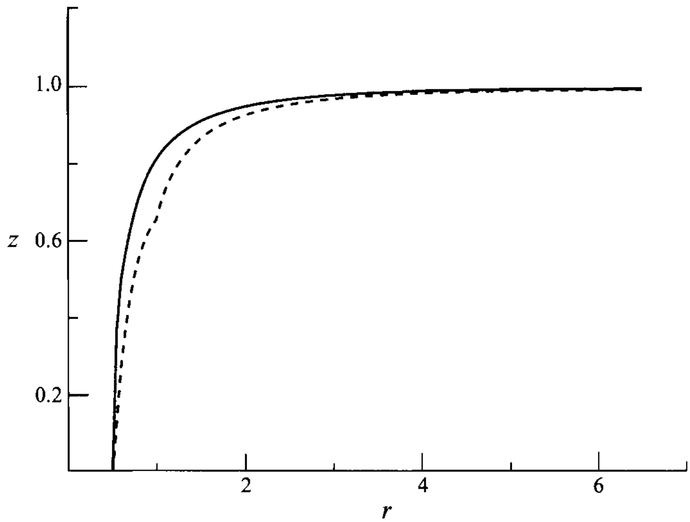

FIGURE 5. A comparison of the surface profiles predicted by the shallow-water approximation (dashed line), and the nonlinear solution (solid line), for the case $\alpha = 1$, $\beta = 0.5$ and $F = 1.8$.

with the full nonlinear solution, however. Eventually, the shallow-water solutions are limited by the constraint (5.6), which is a consequence of the physical restriction that the surface elevation $\zeta(r)$ must be a positive function.

A comparison of the full nonlinear result with the predictions of shallow-water theory is made in figure 5, for the same case as before, in which $\alpha = 1$ and $\beta = 0.5$, and with the Froude number $F = 1.8$. The nonlinear solution is sketched with a solid line, and its Froude number is only about 54% of the maximum value $F_L = 3.3322$ allowed by the theorem of §2. By contrast, the surface computed using the shallow-water formulae (5.3), shown with a dashed line in figure 5, is very close to the limiting configuration allowed in this theory, as required to satisfy the physical constraint $\zeta(r) > 0$; the Froude number $F = 1.8$ used in this diagram is about 86% of the upper bound computed in (5.6). For large Froude numbers, it is clear that the shallow-water theory of §5 under-estimates the surface slope at the drain point $r = \beta$, and also predicts a dimple in the surface at $r = \alpha$, that is not present in the nonlinear profile.

For the results shown in figures 2–5, the inner surface radius β has been held fixed, and the circulation κ computed as part of the solution. Although this strategy is required by the numerical solution scheme, it possibly does not reflect the more usual physical situation, in which the circulation κ is determined by the initial conditions, and the inner radius β found along with the surface shape. Accordingly, the variation of circulation with inner surface radius β has been studied at a fixed Froude number F, and a somewhat surprising result is obtained.

The dependence of circulation κ upon the inner radius β is shown in figure 6, for both the nonlinear case (solid line) as well as for the shallow-water theory (dashed line). In this diagram, the drain radius is $\alpha = 1$, and the Froude number has been fixed at the value $F = 1$. Shallow-water theory predicts a simple linear relation between the circulation and the radius β, as indicated by (5.4), and thus the dashed curve in figure 6 is a straight line with slope $\pi\sqrt{8}$ passing through the origin.

On the other hand, the nonlinear curve in figure 6, sketched with a solid line, indicates that the circulation κ first increases with radius β, reaching a maximum of approximately $\kappa = 5.7$ at about $\beta = 0.75$, before then decreasing rapidly for larger β.

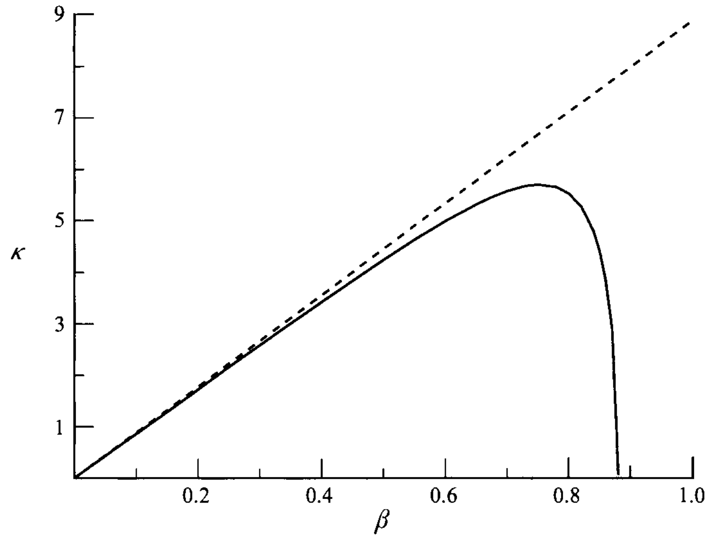

FIGURE 6. The circulation κ as a function of the inner radius β of the free surface at the point of entry into the drain. Here, $\alpha = 1$ and $F = 1$, and the prediction (5.4) of shallow-water theory (dashed line) is compared with the nonlinear solution (solid line).

When the inner radius β is small, the nonlinear circulation κ is in good agreement with the shallow-water result, and increases approximately linearly, as indicated by (5.4). However, it is clear from condition (2.7) and the theorem of §2 that there must be an eventual decrease to zero in the circulation, for a fixed Froude number F, occurring at limiting inner radius β_L given by

$$\beta_L^2 = \alpha^2 - F/(\pi\sqrt{2}).$$

For parameter values $\alpha = 1$ and $F = 1$ used in figure 6, this limiting inner radius is $\beta_L = 0.8803$, and corresponds to the point on the diagram where the solid curve intersects the β-axis.

In a physical experiment, where the circulation κ is likely to be determined in advance (as a result of the initial circulation), there is thus the possibility of genuine non-uniqueness of solutions, since a horizontal line drawn through figure 6 intersects the nonlinear curve twice. This surprising result just follows as a simple consequence of the small Froude number solution (2.11), the theorem of §2, and the intermediate value theorem.

It is significant to observe that the determinant of the Jacobian matrix used in the Newton algorithm in §4 changes sign at the maximum point on the nonlinear curve in figure 6. It is therefore possible that a genuine fold bifurcation takes place at about $(\beta, \kappa) = (0.75, 5.7)$, so that solutions on one side of the maximum are stable, and those on the other side unstable.

Two free-surface profiles are shown in figure 7, for the case $\alpha = 1$, $F = 1$ studied in figure 6. The dashed line represents a solution obtained with $\beta = 0.45$, for which the circulation has been computed to be $\kappa = 3.831$. The other surface profile, drawn with a solid line, corresponds to $\beta = 0.86$, and has circulation $\kappa = 3.819$. Thus for these two solutions the circulation has approximately the same value (differing by only 0.3 %), so that figure 7 essentially illustrates the non-uniqueness of solutions to this problem. It is possible that one of these solutions is physically stable to small disturbances and the

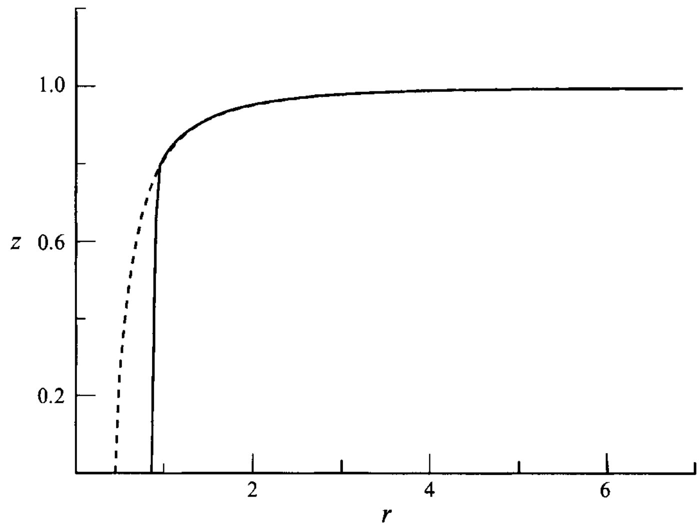

FIGURE 7. Surface profiles for $\alpha = 1$, $F = 1$, at the two different values of the free-surface radius $\beta = 0.45$ (dashed line, $\kappa = 3.831$) and $\beta = 0.86$ (solid line, $\kappa = 3.819$).

other unstable, so that in the laboratory, only one of these outcomes would be realized, for a given circulation.

8. Presentation of results for stagnation-type flow

In addition to the branch of solutions discussed in §7, there is another solution type, having a stagnation point on the surface at $(r, z) = (0, 1)$ and possessing no circulation. Solutions of this type are also known in two-dimensional flows involving a line sink (Hocking & Forbes 1991), and have been computed for three-dimensional flow into a point sink in infinitely deep fluid by Forbes & Hocking (1990). The case of withdrawal into a point sink in fluid of finite depth has been studied by Forbes *et al.* (1993*a*), using a numerical method similar to that outlined in §6.

Two solutions of stagnation type are shown in figure 8, for drain radius $\alpha = 1$. The profile sketched with a dashed line represents a solution obtained with Froude number $F = 1.5$, and the solid line is a solution for $F = 2.385$. The numerical method fails to converge for Froude numbers slightly larger than this value, although some non-physical 'solutions' have been detected at even larger values of F. The determinant of the Jacobian matrix in Newton's method changes sign at about $F = 2.385$, and 'solutions' obtained with larger Froude numbers all possess severe numerical solutions. Consistently with the work of Hocking & Forbes (1991) and Forbes *et al.* (1993*a*), it appears that the failure of the numerical solution at $F = 2.385$ corresponds to the termination of the actual solution branch at approximately this Froude number, and Forbes & Hocking (1993) present evidence that a mathematical singularity may exist at this point. Some small oscillations may be seen in the limiting profile with $F = 2.385$ in figure 8, and these numerically generated features herald the onset of failure of the numerical solution technique.

It has been found in this study that the maximum Froude number at which stagnation-type solutions can occur is strongly dependent on the drain radius α, and this is illustrated in figure 9, where two different limiting solutions are shown, for two

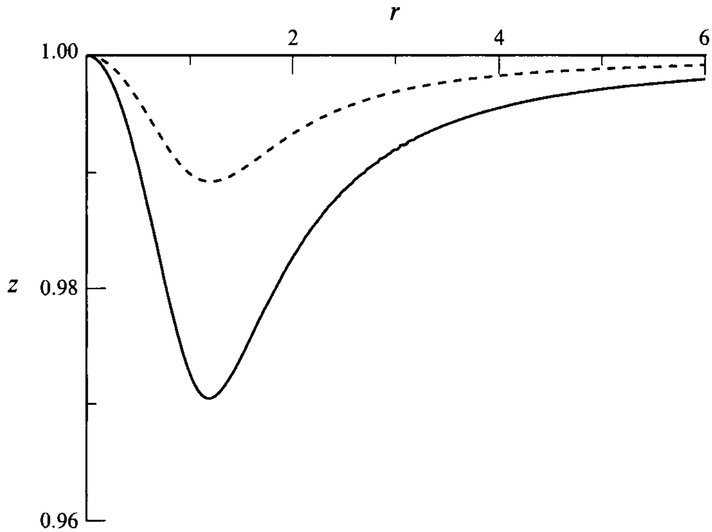

FIGURE 8. Surface profiles of stagnation type, for $\alpha = 1$ and the two values of Froude number $F = 1.5$ (dashed line) and $F = 2.385$ (solid line, limiting case).

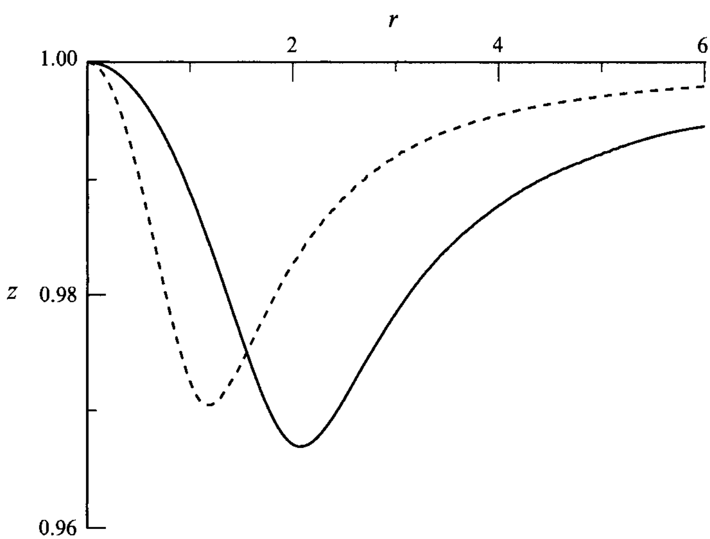

FIGURE 9. Limiting surface profiles of stagnation type, for the two values of drain radius $\alpha = 1$ (dashed line, $F = 2.385$) and $\alpha = 2$ (solid line, $F = 3.90$).

values of α. The profile drawn with a dotted line is the maximal solution with $\alpha = 1$ and $F = 2.385$ shown in figure 8, and the surface sketched with a solid line corresponds to the limiting case for $\alpha = 2$, in which the maximum achievable Froude number has now risen to $F = 3.90$. This is in contrast to the work of Lubin & Springer (1967), who found that the Froude number at which the fluid collapsed into the sink was reasonably insensitive to drain radius, and occurred at about $F \approx 2.53$. Therefore, it is not yet resolved whether the failure of this rather curious branch of stagnation-type solutions is related to the collapse of the free surface into the drain, or not. A similar dilemma exists in the two-dimensional case, where both a stagnation-type solution and a solution possessing a drawn-down cusp at the surface are known, but in which these two solution types are separated by an interval of Froude numbers for which steady solutions have never been obtained. Further discussion of the two-dimensional case is given in Hocking & Forbes (1992).

9. Discussion

In this paper, axisymmetric flow into a circular drain has been investigated. Two distinct solution types have been found, one of which possesses a stagnation point at the free surface and does not involve circulation, and the other for which the surface itself is drawn down into the sink. It has been proved that a limiting Froude number exists for this second type, and that solutions at this maximum value have zero circulation and enter the drain vertically. A numerical solution, based on the method of fundamental singularities, has been used to study the entire solution branch, from zero withdrawal rate ($F = 0$) up to this limiting configuration of maximum Froude number.

The details of the fluid outflow at the drain have been simplified here, by assuming that a constant outflow speed exists. By contrast, Zhou & Graebel (1990) assumed that the normal velocity at the drain varied cubically with radius r across the drain. It is unlikely that the choice of such behaviour has much influence on the qualitative features of the solutions obtained here, although a more realistic description of the outflow velocity distribution might be of interest.

With the aid of the theorem in §2, it has been possible to construct a rather complete understanding of the behaviour of the solution type in which the surface is drawn down into the sink. A one-parameter family of solutions is obtained, in which we have specified the inner surface radius β and computed the circulation κ as an output parameter. In a physical experiment, κ would most likely be determined by initial conditions (and perhaps also by viscous effects at boundaries, although these effects are ignored in this model), and we have found here that *two* different solutions are possible, one of which is presumably stable and the other unstable.

For the other solution type, in which a stagnation point forms at the surface, the situation is somewhat less clear. There is evidently a limiting configuration for these solutions, at some maximum Froude number F, and consistently with the work of Forbes & Hocking (1993) and Forbes *et al.* (1993*a*), the present work suggests the presence of a mathematical singularity at this limiting configuration. However, the maximum Froude number for this branch is strongly dependent upon the drain radius α, whereas the experimental work of Lubin & Springer (1967), for example, indicates that the value of Froude number $F \approx 2.53$ at which the withdrawal layer collapses into the sink is reasonably insensitive to α. It is therefore unclear whether the maximum Froude number found here for this branch of solutions actually corresponds to the sudden collapse of the free surface into the drain.

One advantage of the method of fundamental singularities, used in this paper, is that unsteady calculations can be performed in a relatively straightforward manner, as in Chandler & Forbes (1994). Such a time-dependent approach would possibly clarify the relationship between the two distinct solution branches found here, and indicate which of the two withdrawal-type solutions that exist at the same value of circulation (as in figure 7) is stable. This is worthy of further research.

Most of the computations in this paper were done on a SPARC 10 machine generously supplied by the University of Queensland, under enabling grant R MATHS

UEG-7 93. Collaboration between the investigators has been made possible by University of Western Australia Division of Science small grant 133604, and by the Raybould Bequest to the Department of Mathematics at the University of Queensland, and these are gratefully acknowledged.

Appendix. Potential due to a distributed sink

In this appendix, the potential Φ_0^S is derived, for a single distributed sink lying on the plane $z = 0$ and immersed in an infinite fluid. This is used in § 3 to construct the 'rigid lid' solution Φ^S defined in (3.1), and is central to the present solution technique.

The potential Φ_0^S satisfies Laplace's equation (2.2) in cylindrical polar coordinates. Because this function will be used in (3.3) as part of an infinite sum of image potentials, it is necessary to consider both the lower half-space $z < 0$ in addition to the upper space $z > 0$. Infinitely far away from the sink there is no induced velocity, so all first partial derivatives of Φ_0^S vanish. The boundary condition on the plane $z = 0$ is

$$\begin{aligned} \frac{\partial \Phi_0^S}{\partial z} &= 0 && \text{for} \quad z = 0, \quad \text{and} \quad 0 < r < \beta, \quad r > \alpha, \\ \frac{\partial \Phi_0^S}{\partial z} &= -\frac{F \operatorname{sgn} z}{\pi(\alpha^2 - \beta^2)} && \text{for} \quad z = 0, \quad \beta < r < \alpha, \end{aligned} \tag{A 1}$$

where sgn (z) denotes the sign function of z, as explained following (3.2).

It follows from the assumption of axisymmetry that the solution may be written as a Hankel transform of order zero, in the form

$$\Phi_0^S(r, z) = \int_0^\infty N(k)\, J_0(kr)\, \mathrm{e}^{-k|z|}\, \mathrm{d}k. \tag{A 2}$$

Here, J_0 denotes the Bessel function of order zero, and the weight function $N(k)$ is to be determined so as to satisfy the boundary condition (A 1).

The derivative of (A 2) with respect to z, evaluated on the plane $z = 0$, yields the condition

$$\int_0^\infty kN(k)\, J_0(kr)\, \mathrm{d}k = \begin{cases} C & \text{if } \beta < r < \alpha \\ 0 & \text{otherwise,} \end{cases} \tag{A 3}$$

where, for convenience, the constant $C = F\pi^{-1}(\alpha^2 - \beta^2)^{-1}$ has been defined. In view of the fact that Hankel transforms and their inverses are symmetrical, (A 3) may be inverted to yield the weight function

$$N(k) = \int_\beta^\alpha r J_0(kr)\, C\, \mathrm{d}r.$$

This integral may be evaluated using a standard anti-derivative for Bessel functions (see Abramowitz & Stegun 1972, p. 484), and it then follows that

$$\Phi_0^S(r, z) = \frac{F}{\pi(\alpha^2 - \beta^2)} \int_0^\infty \frac{1}{k} [\alpha J_1(k\alpha) - \beta J_1(k\beta)]\, J_0(kr)\, \mathrm{e}^{-k|z|}\, \mathrm{d}k. \tag{A 4}$$

The induced velocities in (3.2) then follow by taking the radial and vertical derivatives of (A 4).

REFERENCES

ABRAMOWITZ, M. & STEGUN, I. A. (ed.) 1972 *Handbook of Mathematical Functions*. Dover.

CHANDLER, G. A. & FORBES, L. K. 1994 The fundamental solutions method for a free boundary problem. In *Computational Techniques and Applications, Proc. 6th. CTAC, ANU Canberra* (ed. D. Stewart, H. Gardner & D. Singleton), pp. 122–130. World Scientific.

FORBES, L. K. & HOCKING, G. C. 1990 Flow caused by a point sink in a fluid having a free surface. *J. Austral. Math. Soc.* B **32**, 231–249.

FORBES, L. K. & HOCKING, G. C. 1993 Flow induced by a line sink in a quiescent fluid with surface-tension effects. *J. Austral. Math. Soc.* B **34**, 377–391.

FORBES, L. K., HOCKING, G. C. & CHANDLER, G. A. 1993*a* A note on withdrawal through a point sink in fluid of finite depth. *J. Austral. Math. Soc.* B (to appear).

FORBES, L. K., WATTS, A. M. & CHANDLER, G. A. 1993*b* Flow fields associated with in situ mineral leaching. *J. Austral. Math. Soc.* B (to appear).

HOCKING, G. C. 1985 Cusp-like free-surface flows due to a submerged source or sink in the presence of a flat or sloping bottom. *J. Austral. Math. Soc.* B **26**, 470–486.

HOCKING, G. C. 1988 Infinite Froude number solutions to the problem of a submerged source or sink. *J. Austral. Math. Soc.* B **29**, 401–409.

HOCKING, G. C. & FORBES, L. K. 1991 A note on the flow induced by a line sink beneath a free surface. *J. Austral. Math. Soc.* B **32**, 251–260.

HOCKING, G. C. & FORBES, L. K. 1992 Subcritical free-surface flow caused by a line source in a fluid of finite depth. *J. Engng Maths* **26**, 455–466.

IVEY, G. N. & BLAKE, S. 1985 Axisymmetric withdrawal and inflow in a density-stratified container. *J. Fluid Mech.* **161**, 115–137.

JIRKA, G. H. & KATAVOLA, D. S. 1979 Supercritical withdrawal from two-layered fluid systems. Part 2: Three-dimensional flow into round intake. *J. Hydraul. Res.* **17**, 53–62.

LUBIN, B. T. & SPRINGER, G. S. 1967 The formation of a dip on the surface of a liquid draining from a tank. *J. Fluid Mech.* **29**, 385–390.

MILNE-THOMSON, L. M. 1979 *Theoretical Hydrodynamics*, 5th edn. Macmillan.

MILOH, T. & TYVAND, P. A. 1993 Nonlinear transient free-surface flow and dip formation due to a point sink. *Phys. Fluids* A **5**, 1368–1375.

PRUDNIKOV, A. P., BRYCHKOV, YU. A. & MARICHEV, O. I. 1986 *Integrals and Series, Vol. 2: Special Functions* (Translated from Russian by N. M. Queen). Gordon and Breach.

SINGLER, T. J. & GEER, J. F. 1993 A hybrid perturbation-Galerkin solution to a problem in selective withdrawal. *Phys. Fluids* A **5**, 1156–1166.

STROUD, A. H. & SECREST, D. 1966 *Gaussian Quadrature Formulas*. Prentice-Hall.

TUCK, E. O. & VANDEN-BROECK, J.-M. 1984 A cusp-like free-surface flow due to a submerged source or sink. *J. Austral. Math. Soc.* B **25**, 443–450.

ZHOU, Q.-N. & GRAEBEL, W. P. 1990 Axisymmetric draining of a cylindrical tank with a free surface. *J. Fluid Mech.* **221**, 511–532.